

# Design and Analysis of High Performance MEMS Capacitive Pressure Sensor for TPMS

Anil Sharma and Jawar Singh

PDPM-Indian Institute of Information Technology, Design and Manufacturing, Jabalpur

Dumna, Khamaria P.O., Jabalpur, India-482005.

Email: (anil.sharma, jawar)@iiitdmj.ac.in

**Abstract**—In this paper, an analytical and simulation solution has been developed for Micro electromechanical systems (MEMS) based capacitive pressure sensor which finds application in Tyre pressure monitoring system (TPMS). The device simulations, both static and dynamic have been carried out using Intellisuite software. The result shows that, capacitance varies linearly with applied pressure. Its sensitivity came out to be 0.12 fF/KPa within the pressure range of 0-300 KPa. The static results obtained by simulation are in agreement with the theoretical one. The dynamic analysis gives natural frequency and response time of diaphragm.

**Index terms**-MEMS, capacitive pressure sensor, TPMS, Intellisuite

## I. INTRODUCTION

Microelectromechanical systems (MEMS) pressure sensors have gained significant place in the sensor market during last decade. The excellent mechanical properties of silicon combined with the fabrication techniques of integrated circuits have opened up new applications for micromechanical pressure sensors in the past years [6]. Due to various advantages of MEMS pressure sensors like small size, low weight, high pressure sensitivity, and compatibility, it has become the first choice for wide applications in medical, automotive, industrial and aerospace industries.

Automotive industries are the leading consumer of pressure sensors. Typical applications are tyre pressure monitoring system, pressure measurement in gasoline direct injection system, electronic stability program (ESP) gyroscopes and airbags in automotive industries. Tyre pressure monitoring system (TPMS) is highly significant automotive safety equipment required for measuring correct inflation of tyre on road. A Typical TPMS consists of a pressure sensor assembled with microcontrollers and an electronic circuit mounted inside the tyre which continuously monitors the tyre pressure and the information is sent to the driver whether the tyre is correctly inflated or not [8]. In most of the direct TPM systems, MEMS pressure sensors are used. Two types of pressure sensors, piezo-resistive and capacitive are widely used in such applications. Piezo-resistive sensors are highly temperature sensitive, hence they are not preferred. Due to frictional forces, abrupt temperature changes occur inside tyre which affects the performance of sensor. Capacitive pressure sensors are more suitable as they provide very high pressure sensitivity, low noise and very low temperature sensitivity.

Generally, a capacitive pressure sensor is made of two plates which are known as top and bottom electrodes and an air gap or dielectric is placed between these two electrodes. Top electrode is a deformable diaphragm that can be rectangular, square or circular while the bottom electrode is fixed. In a MEMS capacitive pressure sensor, the pressure is applied at top diaphragm keeping bottom electrode as a fixed boundary. Due to this pressure, deformation or deflection occurs at the top diaphragm which will change the effective gap between the two electrodes. This change in effective gap will change the capacitance between two electrodes and this capacitance can be measured by an intermediate electronic circuit [4].

The global TPMS pressure sensor market is expected to grow at a compound annual growth rate (CAGR) of 6.69 percent over the period of 2011-2015. From November 1, 2014, all new passenger cars sold in the European Union must be equipped with TPMS. The increasing demand of such pressure sensors has opened new research trends and various designs are being proposed for such applications. Earlier, proposed sensors were based on simple geometries like circular, rectangular and square. TPMS require highly stable pressure sensor, due to harsh operating environment. Previous designs failed to have high stability. In this paper, we are proposing stepped rectangular diaphragm which is more stable and rigid compared to simply supported or clamped one. To improve other important aspects, i.e., sensitivity and linearity, we have increased the air gap and made the diaphragm thicker as compared to conventional surface micromachined sensors. Earlier, proposed sensors show the capacitance change in the range of aF to fF. This design shows the change in capacitance in the range of pF, which shows better sensitivity and better resolution. Non-linearity at higher pressure range is also minimized[1-9].

## II. DESIGN CONCEPT

The designing of the sensor is done using Intellifab, Fabbviewer and 3D builder modules of Intellisuite software. Surface micro-machining is used to design the capacitive pressure, which makes it CMOS compatible. The virtual fabrication process steps involve growth of sacrificial and structural layer over Si substrate [11]. The sensor is composed of a rectangular polysilicon diaphragm of 5  $\mu\text{m}$  thickness that deflects because of applied normal pressure and acts as the movable plate of a differential capacitor, whereas silicon substrate acts as

a fixed bottom electrode. The distance between deformable diaphragm and substrate material i.e. air gap is  $5 \mu\text{m}$ . The virtual fabrication steps required to design the capacitive pressure sensor is shown in Figure 1.

Initially a PSG layer of thickness  $5 \mu\text{m}$  is deposited over silicon substrate. The mask file to pattern the sacrificial layer, is then created in Intellimask module of Intellisuite software. The dry etching is used to pattern the PSG sacrificial layer. Polysilicon is used as structural (diaphragm) material, which is conformally deposited over the patterned PSG layer. Thickness of the polysilicon layer is kept  $5 \mu\text{m}$ . The rectangular mask file of dimension  $550 \times 450 \mu\text{m}$  is imported from the Intellimask module, and selective etching is used to achieve the stepped profile of the diaphragm. The removal of sacrificial layer is done by applying wet etchant, which creates the desired gap i.e.  $5 \mu\text{m}$  between diaphragm and the base material (substrate).

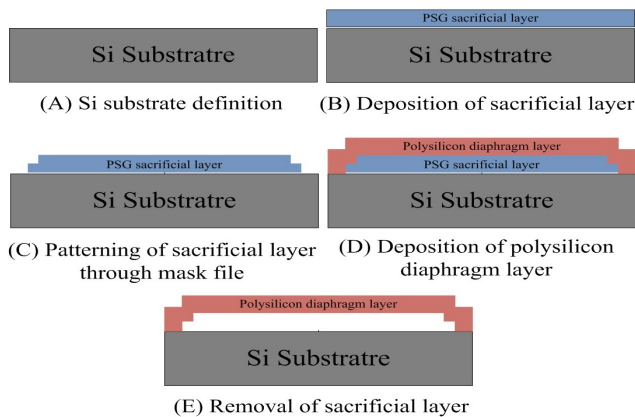


Fig. 1. Virtual fabrication process flow for the designing of capacitive pressure sensor

Rectangular diaphragm shows minimum deflection after applying pressure, compared to circular or square geometries. Stress generated in the rectangular or square diaphragm is more as compared to circular diaphragm, which results in higher sensitivity and makes it suitable for higher pressure range application. Another feature of rectangular diaphragm is its ease of fabrication and better yield [10]. Linearity and sensitivity are very important parameters in design of a pressure sensor. The 3-dimensional view of proposed stepped rectangular diaphragm based pressure sensor is shown in Figure 2.

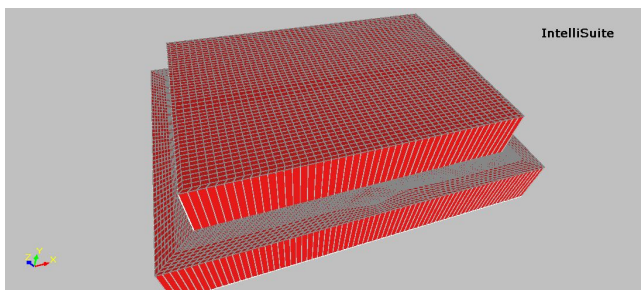


Fig. 2. 3D view of Capacitive Pressure Sensor in Intellisuite

### III. DEFLECTION AND CAPACITANCE ANALYSIS

Our analysis is based on the theory of deflection of thin plates. According to the theory of thin plates, when any diaphragm is subjected to the pressure (lateral, uniform or varying), there will be deflection produced in the diaphragm which will depend upon the different stresses generated in the diaphragm. These stresses will also depend on the type of pressure we are applying. Uniform pressure has been applied on the top surface of the diaphragm. Our diaphragm is a stepped rectangular diaphragm. We are assuming that the weight of the diaphragm is very less i.e. almost negligible compared to other parameters. The length, width and thickness of the diaphragm are in the order of micrometers, due to which the material parameters become very important for the analysis. The basic relation between pressure and deflection is given by the following fourth order differential equation [12]-

$$\left(\frac{\partial^2}{\partial^2 x} + \frac{\partial^2}{\partial^2 y}\right)\left(\frac{\partial^2}{\partial^2 x} + \frac{\partial^2}{\partial^2 y}\right)w = \frac{p}{D} \quad (1)$$

In previous works, different approaches have been proposed for the solution of the above equation, and most of the authors used small deflection theories of plates suggested by Timoshenko [4], [6], [3], and they used this theory for simply supported or clamped diaphragm edges. Here, we have used Naviers approach for the solution of given equation. The deflection profile of the diaphragm is shown in the Figure 3.

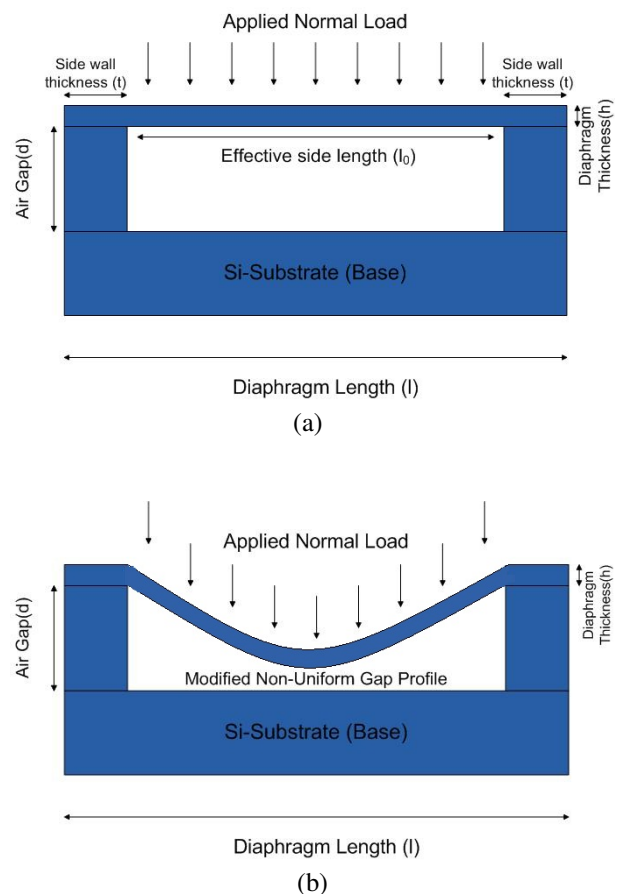


Fig. 3. Schematic of Pressure Sensor (a)when no pressure is applied (b) pressure is applied

The stress distribution profile for the proposed stepped diaphragm based sensor will be different from the simply supported rectangular diaphragm due to its double clamped supported edges. The benefit of using stepped diaphragm is that, it provides more support at the edges, which induces higher stresses at the diaphragm edges and the centre. We have assumed that diaphragm undergoes pure bending and accordingly the boundary conditions are defined.

We have combined the case of pure bending of diaphragm with Naviers approach. Let the diaphragm's length and width at the top surface be  $l$  and  $b$ . As we know that, due to the supported opposite edges, the deflection at the edges will be zero. Hence, the boundary conditions can be defined by the following equations [12]-

$$w = 0, m_{xx} = 0 \quad \text{at } x = 0 \text{ and } x = l_0 \quad (2)$$

$$w = 0, m_{yy} = 0 \quad \text{at } y = 0 \text{ and } y = b_0 \quad (3)$$

where,  $m_{xx}$ ,  $m_{yy}$  are axial bending moments,  $l_0$  and  $b_0$  are inner length and width respectively. Figure 4 shows the inner and outer dimensions of the diaphragm. We have taken Naviers approach for solution of above differential equation. If we assume the pressure function as

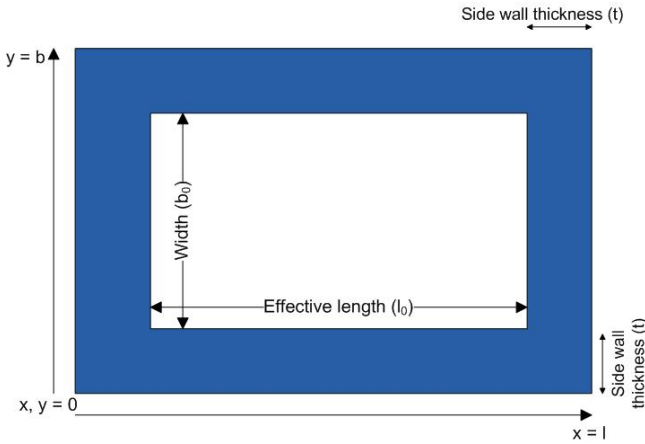


Fig. 4. Co-ordinate system and dimensions of the diaphragm

$$p = f(x, y) \quad (4)$$

where, applied pressure is a function of  $x$  and  $y$ , which is given by the following trigonometric series-

$$f(x, y) = \sum_{m=1}^{\infty} \sum_{n=1}^{\infty} a_{mn} \sin \frac{mx\pi}{l_0} \sin \frac{ny\pi}{b_0} \quad (5)$$

and  $a_{mn}$  is given by the following formula

$$a_{mn} = \frac{4}{l_0 b_0} \int_0^{l_0} \int_0^{b_0} f(x, y) \sin \frac{mx\pi}{l_0} \sin \frac{ny\pi}{b_0} dx dy \quad (6)$$

As we have applied uniform pressure on the top surface of the diaphragm, hence we can take  $f(x,y)$  as a constant and is given by -

$$f(x, y) = p_0 \quad (7)$$

and the above equation can be solved easily and written as-

$$a_{mn} = \frac{4p_0}{l_0 b_0} \int_0^{l_0} \int_0^{b_0} \sin \frac{mx\pi}{l_0} \sin \frac{ny\pi}{b_0} dx dy \quad (8)$$

$$a_{mn} = \frac{16p_0}{\pi^2 mn} \quad (9)$$

Now if we combine the equations (4) and (7) then we can write down the equation for the deflection in the following form-

$$w = \frac{16p_0}{\pi^2 D} \sum_{m=1}^{\infty} \sum_{n=1}^{\infty} \frac{\sin \frac{mx\pi}{l_0} \sin \frac{ny\pi}{b_0}}{mn \left( \frac{m^2}{l_0^2} + \frac{n^2}{b_0^2} \right)^2} \quad (10)$$

Since maximum deflection will be observed at the center and it can be obtained by substituting  $x = \frac{l_0}{2}$  and  $y = \frac{b_0}{2}$  in the equation (8) and is given by the following equation-

$$w_{max.} = 0.00416 \frac{p_0 l_0^4}{D} \quad (11)$$

where

$$\frac{Eh^3}{12(1-\nu^2)} = D = \text{flexural rigidity}$$

In above equation,  $w$  is maximum deflection at center and  $p_0$ ,  $E$ , and  $l_0$  are applied pressure, youngs modulus, poisson's ratio and effective length of the larger side respectively. Due to the non-uniform profile of the diaphragm deflection, gap between top and bottom electrodes will not be constant. So, the capacitance can be calculated by the following equation [3]-

$$C = \iint \frac{\epsilon dx dy}{d - w(x, y)} \quad (12)$$

Above equation shows the non-linearity of capacitance with deflection, this can be solved by using binomial expansion of the denominator. After neglecting the higher order terms, the final expression for the capacitance is given by the following equation [3]-

$$C = C_0 \left( 1 + \frac{1.25pl_0^4}{2025dh} \right) \quad (13)$$

Here  $C_0$  is the zero pressure capacitance and is given by following equation

$$C_0 = \frac{0.4\epsilon l_0^4}{d} \quad (14)$$

and the sensitivity can be given by following equation-

$$S_A = \frac{dC}{dP} \quad (15)$$

$$S_A = C_0 \left( \frac{1.25l_0^4}{2025dh} \right) \quad (16)$$

#### IV. RESULTS AND DISCUSSION

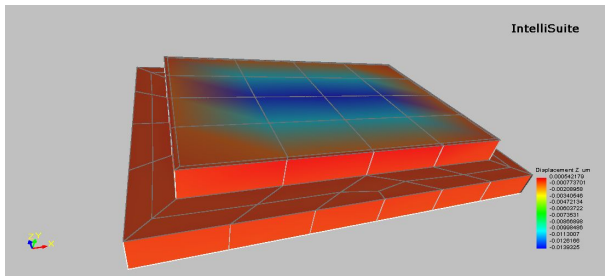
Finite element analysis of the model is performed using thermo-electro mechanical (TEM) tool of Intellisuite. Static and dynamic analysis is done. Table 1 shows the diaphragm parameters which are considered during simulation and analysis. Thermoelctromechanical relaxation is performed for static analysis.

The pressure range varies from 0 to 300 KPa. The standard pressure of a car tyre is 242. Hence considerable pressure range lie between 230-270 KPa. The corresponding maximum

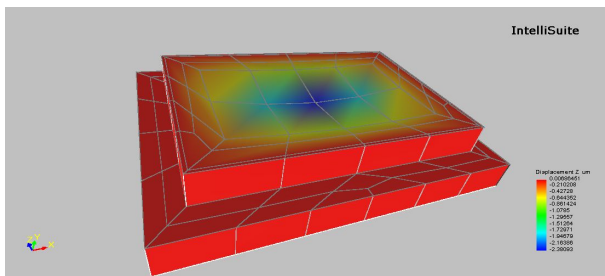
TABLE I  
STRUCTURAL PARAMETERS OF SENSOR

Young's modulus[ $E$ ]	169 GPa
Poisson's ratio[ $\nu$ ]	0.22
Density	2.32 gram/cm <sup>3</sup>
Effective side length[ $l_0$ ]	450 $\mu$ m
Air gap[ $d$ ]	5 $\mu$ m
Diaphragm thickness[ $h$ ]	5 $\mu$ m
Residual stress	10 MPa

deflection at center varies up to 2.5  $\mu$ m for the maximum pressure range. Figure 3(a) and 3(b) shows the deflection of the diaphragm (when the residual stress is 10 MPa) at pressure of 0 KPa and 300 KPa correspondingly. In figure 4, the comparative analysis is done when the residual stress present in diaphragm is 0 MPa and 10 MPa along with the theoretical results. This residual stress is produced in the diaphragm due to the non-uniformity of the deposition process and the mismatch of the material properties of substrate and the diaphragm material.



(a)



(b)

Fig. 5. (a) Deflection at 0 KPa (b) Deflection at 300 KPa

As the deflection is limited to the 45% of the diaphragm thickness, the deflection pressure curve (figure 4) shows excellent linearity in its full scale, which is highly desirable for various application. Due to the non-uniform profile of diaphragm deflection, the capacitance will not be a constant function of the air gap. Figure 5 shows the pressure capacitance relation for the pressure range 0-300 KPa along with the theoretical results obtained from the analytical formula. The pressure capacitance curve shows better linearity at higher pressure. Thus, the sensitivity becomes almost constant between pressure range of 200 to 300 Kpa, as the standard pressure of a tyre is almost 242 Kpa. Hence, linearity in this range is highly desirable.

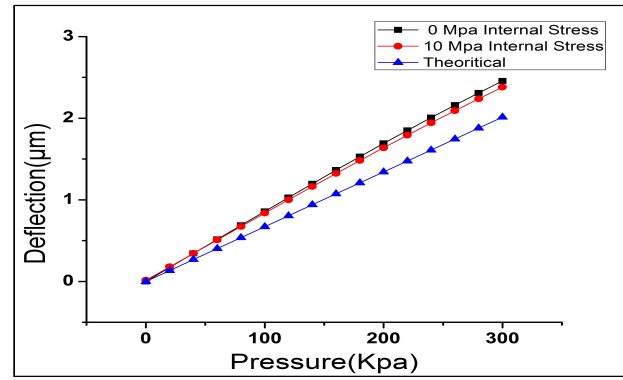


Fig. 6. Pressure Deflection Relationship

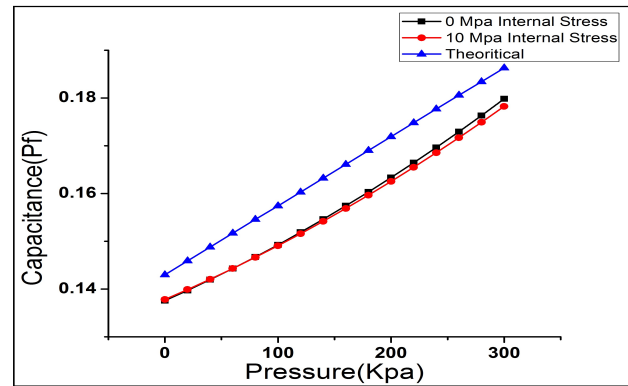


Fig. 7. Pressure Capacitance Relationship

The simulated sensitivity in full scale is almost 0.120 fF/KPa, whereas the calculated sensitivity is 0.145 fF/KPa, and the maximum non-linearity present in the curve (figure 5) is almost 8%.

Dynamic analysis is performed for frequency and time response of the diaphragm. In addition to the static pressure requirements, the frequency response of the sensor must be considered [13]. As the diaphragm behaves like a spring mass system, hence its dynamic response depends on its stiffness, mass and the degree of damping present. Natural frequency is the frequency at which the system vibrates naturally once it has been set into motion. The simulation is done in the frequency range of 2 MHz to 9 MHz. From Figure 6, it can be seen that the highest natural mode frequency for the diaphragm is 3 MHz. At 3 MHz, diaphragm shows maximum vibration. Hence variable pressure of 3 MHz frequency should be avoided as it may break the diaphragm.

For time-displacement analysis, an input pulse for the time period of 3 microseconds is applied. Figure 7 shows the graph between time and displacement which represents the settling time for the diaphragm to settle down after applying step input, the observed settling time is .055 millisecond (Figure 7). The time-displacement and frequency-displacement dynamic analysis curve shows the better stability and compatibility of the pressure sensor.

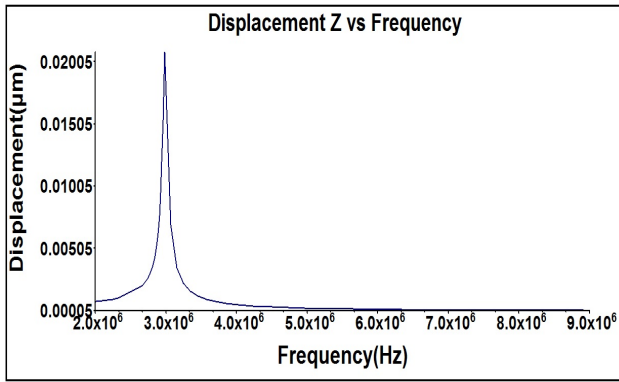


Fig. 8. Dynamic Analysis Curve (Displacement vs Frequency)

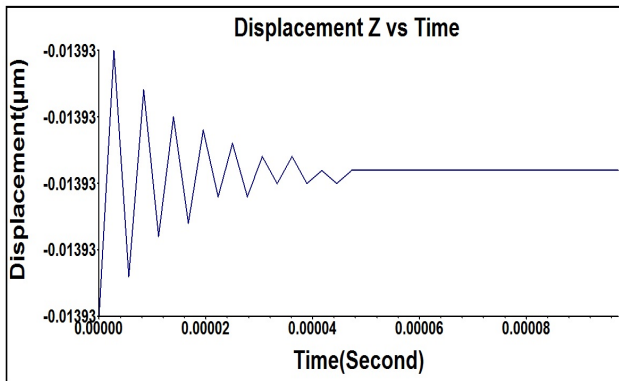


Fig. 9. Dynamic Analysis Curve (Displacement vs Time)

## V. CONCLUSION

A high performance MEMS capacitive pressure sensor for TPMS has been designed and simulated. A stepped rectangular diaphragm with higher thickness i.e.  $5 \mu\text{m}$  has been used to achieve absolute linearity for pressure deflection. The gap has been made  $5 \mu\text{m}$  to reduce non-linearity of capacitance curve. The rate of change of deflection is higher which also changes the capacitance with higher rate. This, in turn, increases the sensitivity of the sensor. The natural frequency in the range of MHz ensures its higher stability.

## REFERENCES

- [1] E. G. Bakhoun and M. H. Cheng. Capacitive pressure sensor with very large dynamic range. *IEEE Transactions on Components and Packaging Technology*, 33(1), mar.2010.
- [2] J. D. C. A. Z. Darrin J, Young and W. H. Ko. High-temperature single crystal 3c-sic capacitive pressure sensor. *IEEE Sensors Journal*, 4(4):464–470, 2004.
- [3] A. S. Deepika, Manju Mittal. Virtual prototyping of a mems capacitive pressure sensor for tpms using intellisuite. In *International Symposium on Physics and Technology of Sensors*, pages 25–28. IEEE, 2012.
- [4] P. Eswaran and S. Malarvizhi. Design analysis of mems capacitive differential pressure sensor for aircraft altimeter. *International Journal of Applied Physics and Mathematics*, 2(1), jan.2012.
- [5] M. K. R. K. C. Katuri and S. Asrani. A surface micromachined capacitive pressure sensor for intraocular pressure measurement. In *ASME International Conference on Mechatronics and Embedded Systems and Applications*, pages 149–154. IEEE, 2010.
- [6] H.-C. C. Liwei Lin and Y.-W. Lu. A simulation program for the sensitivity and linearity of piezoresistive pressure sensors. *Journal of Microelectromechanical Systems*, 8(4), dec.1999.

- [7] B. A. G. M. Shahiri-Tabarestani and R.Sabbaghi-Nadooshan. Design and simulation of high sensitive capacitive pressure sensor with slotted diaphragm. In *International Conference on Biomedical Engineering, Penang*, pages 484–489, 2012.
- [8] M. G. Michael PAINE and N. MAGEDARA. *The Role of Tyre Pressure in Vehicle Safety, Injury and Environment*. Road Safety Solutions, 2007.
- [9] A. V. J. S. Sathyanarayana. Design and simulation of touch mode mems capacitive pressure sensor. In *International Conference on Mechanical and Electrical technology*. IEEE, 2010.
- [10] A. sharma and P. George. A simple method for calculation of pull-in voltage and touch point pressure for the small deflection of square diaphragm in mems. *ScienceDirect, Sensors and Actuators, A* 141:376–382, 2008.
- [11] stephen beby and graham ensell. *MEMS Mechanical Sensors*. artech house, inc., boston, london, 2004.
- [12] S. Timoshenko. *Theory of Plates and Shells*. Mcgraw-hill, new york, 1986.
- [13] T. M. Xine Li, Jing Zu and PengXu. Research on novel capacitive pressure sensor to measure chamber pressures of different caliber artilleries. *IEEE Sensors Journal*, 11(4), apr.2011.
- [14] B. G. Y. Zhang, R. Howver and N. Yazdi. A high-sensitive ultra-thin mems capacitive pressure sensor. In *Actutors and Microsystems Conference, Beijing*, pages 112–115. IEEE, 2011.